AFRL-AFOSR-VA-TR-2022-0131

Risk Analysis of Stochastic Nonlinear Dynamical Networks via Lifting Operators

Motee, Nader
LEHIGH UNIVERSITY
526 BRODHEAD AVE
BETHLEHEM, PA, 18015
USA

04/11/2022
Final Technical Report

Air Force Research Laboratory
Air Force Office of Scientific Research
Arlington, Virginia 22203
Air Force Materiel Command

REPORT DOCUMENTATION PAGE

PLEASE DO NOT RETURN YOUR FORM TO THE ABOVE ORGANIZATION.

1. REPORT DATE	2. REPORT TYPE	3. DATES COVERED	
20220411	Final	START DATE 20181101	END DATE 20211031

4. TITLE AND SUBTITLE
Risk Analysis of Stochastic Nonlinear Dynamical Networks via Lifting Operators

5a. CONTRACT NUMBER	5b. GRANT NUMBER	5c. PROGRAM ELEMENT NUMBER
	FA9550-19-1-0004	61102F
5d. PROJECT NUMBER	**5e. TASK NUMBER**	**5f. WORK UNIT NUMBER**

6. AUTHOR(S)
Nader Motee

7. PERFORMING ORGANIZATION NAME(S) AND ADDRESS(ES)
LEHIGH UNIVERSITY
526 BRODHEAD AVE
BETHLEHEM, PA 18015
USA

8. PERFORMING ORGANIZATION REPORT NUMBER

9. SPONSORING/MONITORING AGENCY NAME(S) AND ADDRESS(ES)	10. SPONSOR/MONITOR'S ACRONYM(S)	11. SPONSOR/MONITOR'S REPORT NUMBER(S)
Air Force Office of Scientific Research 875 N. Randolph St. Room 3112 Arlington, VA 22203	AFRL/AFOSR RTA2	AFRL-AFOSR-VA-TR-2022-0131

12. DISTRIBUTION/AVAILABILITY STATEMENT
A Distribution Unlimited: PB Public Release

13. SUPPLEMENTARY NOTES

14. ABSTRACT
In this project, we developed operator theoretic tools to study convergence of Carleman lifting of time-varying nonlinear systems. We quantified explicit error bounds for finite-section of the lifted system and proved that the truncation error converges exponentially to zero as the truncation length increases. We utilized our findings to study Hamilton-Jacobi-Bellman (HJB) equation and proposed a quadrization method to lift and represent the HJB equation as a semi-Riccati operator equation. An exact iterative algorithm to calculate the sub-blocks of the solution to the semi-Riccati operator equation up to an arbitrary precision was proposed. Furthermore, we developed a methodology to study and quantify systemic risk measures in various dynamical networks subject to Gaussian or stable non-Gaussian noise. More specifically, our findings show that for a class of nonlinear dynamical networks one can quantify the value of a family of risk measures using spectral mode decomposition techniques. Our theoretical results have been applied to various applications including platoon of autonomous vehicles, swarm of multiple robots, rendezvous and synchronization in multi-agent systems, and power networks.

15. SUBJECT TERMS

16. SECURITY CLASSIFICATION OF:			17. LIMITATION OF ABSTRACT	18. NUMBER OF PAGES
a. REPORT U	b. ABSTRACT U	c. THIS PAGE U	UU	19

19a. NAME OF RESPONSIBLE PERSON	19b. PHONE NUMBER *(Include area code)*
FREDERICK LEVE	696-9730

Final Report FA9550-19-1-0004

Risk Analysis of Stochastic Nonlinear Dynamical Networks via Lifting Operators

Program Manager: Dr. Frederick A. Leve
Principle Investigator: Nader Motee
Institution: Lehigh University
Start Date: 01 November 2018
Report Date: 31 October 2021

Number of Journal Papers: 14 journal papers (9 published/accepted and 5 under review)
Number of Conference Papers: 13 conference papers (8 published and 5 under review)

Abstract

In this project, we developed operator theoretic tools to study convergence of Carleman lifting of time-varying nonlinear systems. We quantified explicit error bounds for finite-section of the lifted system and proved that the truncation error converges exponentially to zero as the truncation length increases. We utilized our findings to study Hamilton-Jacobi-Bellman (HJB) equation and proposed a quadrization method to lift and represent the HJB equation as a semi-Riccati operator equation. An exact iterative algorithm to calculate the sub-blocks of the solution to the semi-Riccati operator equation up to an arbitrary precision was proposed. Furthermore, we developed a methodology to study and quantify systemic risk measures in various dynamical networks subject to Gaussian or stable non-Gaussian noise. More specifically, our findings show that for a class of nonlinear dynamical networks one can quantify the value of a family of risk measures using spectral mode decomposition techniques. Our theoretical results have been applied to various applications including platoon of autonomous vehicles, swarm of multiple robots, rendezvous and synchronization in multi-agent systems, and power networks.

1 Accomplishments

The technical accomplishments of this project have been disseminated through 14 journal papers and 13 papers in conference proceedings. A complete list of publications can be found in the reference section of this report. Some of these papers have been published or in press and some are still under review. In this report, we only focus on some of the major accomplishments in the area of nonlinear dynamical and control systems. We will briefly discuss the remaining achievements and provide reference for further details. Our main contributions include:

- Quantifying explicit error bounds and convergence conditions for finite-section of Carleman linearization of a broad class of time-varying nonlinear systems [4, 7, 10]
- Proposing a methodology to exploit inherent structure of nonlinear systems and equations to reduce their computational complexities and enable tractable optimal design procedures [5, 7]
- Formulating a semi-Riccati operator equation to exploit inherent structure of the well-known Hamilton-Jacobi-Bellman (HJB) equation and proposing an exact iterative method to solve it with arbitrary precision [5, 6]
- Proposing a quadrization procedure to lift the HJB equation that can be similarly applied to the Fokker-Planck equation for risk analysis of stochastic nonlinear systems [5, 6]
- Quantifying risk measures for a class of nonlinear dynamical systems using Koopman modes decomposition [22]
- Quantifying risk measures for a class of linear dynamical networks driven by Gaussian or stable non-Gaussian disturbances [26, 16, 11, 12, 21, 24]
- Quantifying risk measure for platoon of autonomous vehicles and synchronous power networks in presence of time-delay and characterizing fundamental limits and tradeoffs on the best achievable levels of risk in these applications [23, 20, 27, 25, 18]
- Proposing risk-aware learning algorithms for recurrent neural networks and their applications in multi-agent systems [1, 13, 17, 2, 15, 14]
- Exploiting sparsity in stability verification and sampling in networked control systems [19, 3]
- Statistical learning of nonlinear dynamical networks using a single trajectory [9, 8]

1.1 Lifting of Nonlinear Dynamical Systems

In his 1932 paper, Carleman proposed a linearization method to transform a given finite-dimensional nonlinear system with analytic right-hand into an equivalent infinite-dimensional linear system with (usually) unbounded operators. Finite truncation of the transformed system has been used to study dynamic properties, learning, and control of nonlinear systems. One of the remaining outstanding problems in this context is quantifying the effectiveness of such finitely truncated models. Intuitively, one expects that as the truncation length increases, the truncated system will approximate the original nonlinear more effectively. In this part of the project, we provide explicit error bounds and prove that the trajectory of the truncated system stays close to that of the original nonlinear system over a quantifiable time interval. We also show that the error bounds converge exponentially to zero by increasing the truncation length. This is particularly important in applications, such as Model Predictive Control, to choose proper truncation lengths for a given sampling period and employ the

resulting truncated system as a good approximation of the nonlinear system. The details of research achievements in this part can be found in references [7, 10].

1.1.1 Carleman Linearization

In this project, we consider the class of nonlinear systems whose dynamics are governed by

$$\dot{\mathbf{x}} = \mathbf{f}(t, \mathbf{x}) \tag{1.1}$$

for all $t \geq t_0$ with a nonzero initial condition $\mathbf{x}(t_0) = \mathbf{x}_0$, at a neighborhood of its equilibrium at the origin, where the state of the system is denoted by $\mathbf{x} = [x_1, \ldots, x_d]^T \in \mathbb{R}^d$ and the components of function

$$\mathbf{f}(t, \mathbf{x}) = \big[f_1(t, \mathbf{x}), \ldots, f_d(t, \mathbf{x})\big]^T$$

for $t \geq t_0$, are analytic on a neighborhood of the equilibrium. Without loss of generality, it is assumed that $\mathbf{f}(t, \mathbf{0}) = \mathbf{0}$. For a given multi-index vector $\boldsymbol{\alpha} = [\alpha_1, \ldots, \alpha_d]^T \in \mathbb{Z}_+^d$, let us define $\mathbf{x}_{\boldsymbol{\alpha}} = x_1^{\alpha_1} \cdots x_d^{\alpha_d}$ and express the Maclaurin series expansion of the vector-valued function $\mathbf{f}(t, \mathbf{x})$ by

$$\mathbf{f}(t, \mathbf{x}) = \sum_{\boldsymbol{\alpha} \in \mathbb{Z}_+^d \setminus \{\mathbf{0}\}} \mathbf{f}_{\boldsymbol{\alpha}}(t) \mathbf{x}_{\boldsymbol{\alpha}} \tag{1.2}$$

in which $\mathbf{f}_{\boldsymbol{\alpha}}(t) = [f_{1,\boldsymbol{\alpha}}(t), \ldots, f_{d,\boldsymbol{\alpha}}(t)]^T$. The conventional Carlemen linearization of the nonlinear dynamic system (1.1) starts from the reformulation

$$\dot{x}_j = \sum_{\alpha \in \mathbb{Z}_+^d \setminus \{\mathbf{0}\}} f_{j,\alpha}(t)\, \mathbf{x}_{\boldsymbol{\alpha}} \tag{1.3}$$

for every $j = 1, \ldots, d$. The standard Euclidean basis for $\mathbb{R}^d$ is denoted by $\mathbf{e}_j = [0, \cdots, 0, 1, 0, \cdots, 0]^T$ for $j = 1, \ldots, d$ and it is assumed that

$$f_{j,\boldsymbol{\alpha}} = 0 \;\text{ if }\; \boldsymbol{\alpha} \notin \mathbb{Z}_+^d \setminus \{\mathbf{0}\}. \tag{1.4}$$

Let us define $|\boldsymbol{\alpha}| = \alpha_1 + \cdots + \alpha_d$ for $\boldsymbol{\alpha} = [\alpha_1, \ldots, \alpha_d]^T \in \mathbb{Z}_+^d$ and

$$\mathbb{Z}_k^d = \Big\{ \boldsymbol{\alpha} \in \mathbb{Z}_+^d \;\Big|\; |\boldsymbol{\alpha}| = k \Big\}$$

for $k \geq 0$. By regrouping all $\boldsymbol{\alpha} \in \mathbb{Z}_k^d$ for every $k \geq 1$ and defining $\mathbf{z}_k = \big[\mathbf{x}_{\boldsymbol{\alpha}}\big]_{\boldsymbol{\alpha} \in \mathbb{Z}_k^d}$, we can represent the original nonlinear system in terms of $\mathbf{z}_k$'s and obtain the following infinite-dimensional linear dynamical system

$$\dot{\mathbf{z}}_k = \sum_{l=k}^{\infty} \mathbf{A}_{k,l}(t)\, \mathbf{z}_l \tag{1.5}$$

for all $t \geq t_0$ and $k \geq 1$ with initial condition $\mathbf{z}_k(t_0) = \big[\mathbf{x}_{\boldsymbol{\alpha}}^0\big]_{\boldsymbol{\alpha} \in \mathbb{Z}_k^d}$, where

$$\mathbf{A}_{k,l}(t) = \left[\sum_{j=1}^{d} \alpha_j f_{j,\boldsymbol{\beta}-\boldsymbol{\alpha}+\mathbf{e}_j}(t) \right]_{\boldsymbol{\alpha} \in \mathbb{Z}_k^d,\ \boldsymbol{\beta} \in \mathbb{Z}_l^d} \tag{1.6}$$

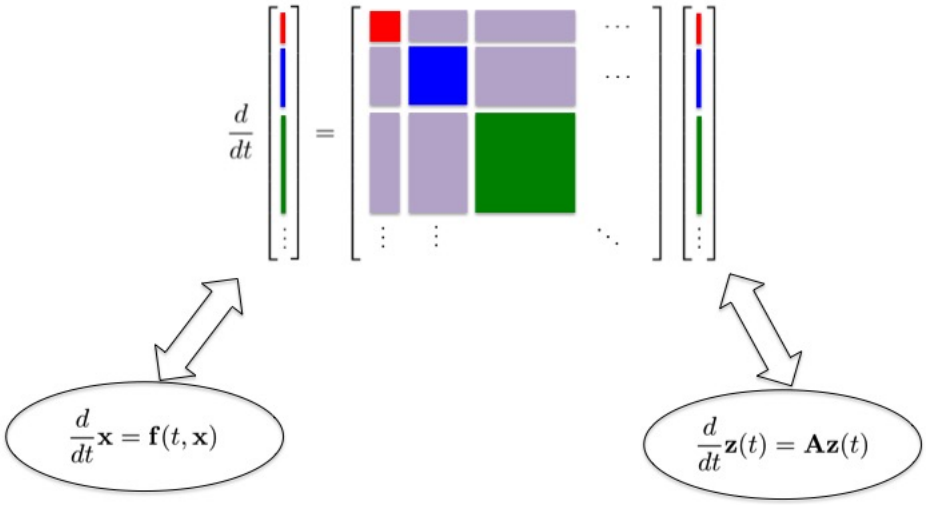

for all $k, l \geq 1$ are matrices of size $\binom{k+d-1}{d-1} \times \binom{l+d-1}{d-1}$. By defining the infinite-dimensional state vector $\mathbf{z} = \left[\mathbf{z}_1, \mathbf{z}_2, \ldots, \mathbf{z}_N, \ldots\right]^T$, the set of linear systems (1.5) can be rewritten in compact form

$$\dot{\mathbf{z}} = \mathbf{A}(t)\mathbf{z} \tag{1.7}$$

for $t \geq t_0$ with initial condition $\mathbf{z}(t_0) = \left[\mathbf{x}_{\boldsymbol{\alpha}}^0\right]_{\boldsymbol{\alpha} \in \mathbb{Z}_+^d \setminus \{\mathbf{0}\}}$, where

$$\mathbf{A}(t) = \begin{bmatrix} \mathbf{A}_{1,1}(t) & \mathbf{A}_{1,2}(t) & \cdots & \mathbf{A}_{1,N}(t) & \cdots \\ & \mathbf{A}_{2,2}(t) & \cdots & \mathbf{A}_{2,N}(t) & \cdots \\ & & \ddots & \vdots & \ddots \\ & & & \mathbf{A}_{N,N}(t) & \cdots \\ & & & & \ddots \end{bmatrix} \tag{1.8}$$

is a block upper-triangular matrix. The resulting linear system (1.7) is referred to as the *Carleman linearization* of the nonlinear dynamical system (1.1).

While the original d-dimensional dynamical systems (1.1) is nonlinear, its lifted form (1.5) is an infinite-dimensional linear system whose state matrix $\mathbf{A}$ is an upper-triangular block matrix with special structure and initial condition is of exponential type. On the other hand, the apparent disadvantage of the Carleman linearization is that the resulting state matrix $\mathbf{A}$ is not a bounded operator on $\ell^2(\mathbb{Z}_+^d \setminus \{\mathbf{0}\})$, the Hilbert space of all square-summable sequences on $\mathbb{Z}_+^d \setminus \{\mathbf{0}\}$. Moreover, the initial condition has exponential decay when $\|\mathbf{x}_0\| < 1$ and exponential growth when $\|\mathbf{x}_0\| > 1$, which prevents the direct application of existing theories to analyze the infinite-dimensional linear system on Hilbert spaces $\ell^2(\mathbb{Z}_+^d \setminus \{\mathbf{0}\})$.

A natural question about the original nonlinear system (1.1) and its Carleman linearization (1.5) is:

How effective the finite-section (truncation) of the linearized counterpart is and whether the first component of the solution of the truncated system converges to the solution of the original nonlinear system.

Our main contribution shows that if the convergence radius of function $\mathbf{f}(t, \mathbf{x})$ is finite, then the finite-section of the Carlemen linearization converges exponentially to the solution of the original nonlinear system in a neighborhood of the equilibrium. A significant implication of our result is that Carlemen linearization can be used for short-time state prediction in nonlinear dynamical systems.

1.1.2 Convergent Finite-Section Approximations

In this project, we show that the first component of the solution of the finite-section approach to the Carlemen linearization converges to the solution of the original nonlinear dynamical system (1.1) exponentially when the initial condition is not too far away from the equilibrium. The N'th order finite-section of the Carlemen linearization (1.7) is linear system

$$\begin{bmatrix} \dot{\mathbf{y}}_{1,N}(t) \\ \dot{\mathbf{y}}_{2,N}(t) \\ \vdots \\ \dot{\mathbf{y}}_{N,N}(t) \end{bmatrix} = \begin{bmatrix} \mathbf{A}_{1,1}(t) & \mathbf{A}_{1,2}(t) & \cdots & \mathbf{A}_{1,N}(t) \\ & \mathbf{A}_{2,2}(t) & \cdots & \mathbf{A}_{2,N}(t) \\ & & \ddots & \vdots \\ & & & \mathbf{A}_{N,N}(t) \end{bmatrix} \begin{bmatrix} \mathbf{y}_{1,N}(t) \\ \mathbf{y}_{2,N}(t) \\ \vdots \\ \mathbf{y}_{N,N}(t) \end{bmatrix} \tag{1.9}$$

with dimension $d\binom{N+d}{d} - d$ and initial $\mathbf{y}_{k,N}(t_0) = \left[\mathbf{x}_0^{\boldsymbol{\alpha}}\right]_{\boldsymbol{\alpha} \in \mathbb{Z}_k^d}$ for all $1 \le k \le N$.

Assumption 1.1. The function $\mathbf{f}(t, \mathbf{x})$ in (1.1) is a time-varying analytic function near the origin such that $\mathbf{f}(t, \mathbf{0}) = \mathbf{0}$ for all $t \ge t_0$ and coefficients $\mathbf{f}_{\boldsymbol{\alpha}}(t)$ in its Marclaurin expansion (1.2) satisfy uniform exponential decay property

$$\sup_{t \ge t_0} \sum_{j=1}^{d} \sum_{\boldsymbol{\alpha} \in \mathbb{Z}_k^d} |f_{j,\boldsymbol{\alpha}}(t)| \le D_0 R^{-k} \tag{1.10}$$

for all $k \ge 1$ and some positive constants D_0 and R.

This assumption is reasonable as almost all the common functions appearing in various applications satisfy this decay requirement.

Theorem 1.1. *Suppose that Assumption 1.1 holds and $\mathbf{x}(t)$ for $t \ge t_0$ is a continuous solution of the nonlinear system* (1.1) *with initial condition $\mathbf{x}(t_0) = \mathbf{x}_0$ that satisfies*

$$0 < \|\mathbf{x}_0\|_\infty < \frac{R}{e}. \tag{1.11}$$

Then, the first component of the solution of the finite section of the Carleman linearization (1.9)*, i.e., $\mathbf{y}_{1,N}(t)$, converges to $\mathbf{x}(t)$ exponentially as the truncation length N increases for all $t_0 \le t < t_0 + T^*$. More specifically, for every $t_0 < t_1 < t_0 + T^*$, there exist a positive constant C such that*

$$\sup_{t_0 \le t \le t_1} \|\mathbf{y}_{1,N}(t) - \mathbf{x}(t)\|_\infty \le C\, e^{D_0(t_1 - t_0 - T^*)N/R} \tag{1.12}$$

for all $N \ge 1$, where

$$T^* = \frac{(e-1)R}{(2e-1)D_0} \ln\left(\frac{R}{e\|\mathbf{x}_0\|_\infty}\right). \tag{1.13}$$

The convergence of the finite-section scheme has been studied before when the right-hand side of the nonlinear system (1.1) is a time-varying polynomial

$$\mathbf{p}_L(t,\mathbf{x}) = \sum_{1\leq|\boldsymbol{\alpha}|\leq L} \mathbf{p}_{\boldsymbol{\alpha}}(t)\mathbf{x}^{\boldsymbol{\alpha}} \tag{1.14}$$

with degree $L \geq 1$, where $\mathbf{p}_{\boldsymbol{\alpha}}(t) = \big[p_{1,\boldsymbol{\alpha}}(t),\ldots,p_{d,\boldsymbol{\alpha}}(t)\big]^T$. If $L = 1$, it can be verified that the corresponding state matrix $\mathbf{A}(t)$ in the Carlemen linearization (1.8) will be a block diagonal matrix. Hence, the first component $\mathbf{y}_{1,N}(t)$ of the solution of the finite section scheme (1.9) will be equal to the continuous solution $\mathbf{x}(t)$ for all $t \geq t_0$ of the original nonlinear dynamic system (1.1). To verify usefulness of our theoretical findings, we consider the case where the degree of the polynomial $\mathbf{P}_L$ is at least two, i.e., $L \geq 2$. We define quantity

$$D_0(\mathbf{p}_L,R) = \sup_{1\leq k\leq L} R^k \sup_{t\geq t_0} \sum_{j=1}^{d} \sum_{\boldsymbol{\alpha}\in\mathbb{Z}_k^d} |p_{j,\boldsymbol{\alpha}}(t)| \tag{1.15}$$

for $R > 0$. For all convergence radius $R > 0$, the uniform exponential decay property (1.10) holds for the time-varying polynomial $\mathbf{p}_L(t,\mathbf{x})$ with D_0 replaced by $D_0(\mathbf{p}_L,R)$, and for any nonzero initial $\mathbf{x}_0$, the requirement (1.11) is satisfied when R is chosen appropriately. Therefore, as a byproduct of Theorem 1.1, we obtain the following result.

Theorem 1.2. *Let us consider the nonlinear dynamical system* (1.1) *whose right-hand side is given by the time-varying polynomial* (1.14) *with* $L \geq 2$. *Then, the solution* $\mathbf{y}_{1,N}(t)$ *of the truncated system* (1.9) *converges to the solution* $\mathbf{x}(t)$ *of the original nonlinear dynamic system* (1.1) *over time interval for all* $t_0 < t < t_0 + T^*$, *where*

$$T^* = \frac{(e-1)(L-1)}{(2e-1)e^{L^2-L}\left(\sup_{t\geq t_0}\sum_{j=1}^{d}\sum_{\boldsymbol{\alpha}\in\mathbb{Z}_L^d}|p_{j,\boldsymbol{\alpha}}(t)|\right)}\ \|\mathbf{x}_0\|_\infty^{1-L}.$$

Several lemmas and theorems have been proved to pave the way for the proof of Theorem 2.1, which is rather technical and detailed. To improve readability of this report, we omitted all the technical steps, which can be found in [7, 10].

1.2 Quadratization of the HJB Equation and Its Exact Sequential Approximations

In this part of the project, we propose a novel tractable approximate solution to the classical optimal control problem of a nonlinear control system and its corresponding Hamilton-Jacobi-Bellman (HJB) equation. Our focus is on systems whose right-hand sides are analytic functions, i.e., they admit power series representations. We utilize quadratization techniques to lift the HJB equation, which is a nonlinear partial differential equation, into an operator equation that resembles the well-known Riccati equation. We exploit the structural properties of this operator equation to calculate the block components of its solution using an *exact* iterative method. The uniqueness of the solution is proven and it is shown that under some technical assumptions the resulting closed-loop system is stable in the sense of Lyapunov. We show that one only needs to run finitely many iterations to compute a stabilizing near-optimal solution for the optimal control problem. The details of research achievements in this part can be found in references [4, 6, 5].

1.2.1 Bilinearization of the Nonlinear Control System

We consider the class of nonlinear control systems

$$\dot{x} = f(x) + g(x)u, \tag{1.16}$$

where $f, g : \mathbb{R}^n \to \mathbb{R}^n$ are smooth functions, $x \in \mathbb{R}^n$ is the state pf the system, and $u \in \mathbb{R}$ is the scalar control input. It is assumed that maps f and g are analytic in a neighborhood of the origin and $f(0) = 0$, i.e., $x = 0$ is an equilibrium point of (1.16) when input is identically zero.

The classical optimal control problem is to find a control law that minimizes the cost functional

$$J(x, u) = \int_0^\infty \big[q(x(t)) + ru^2(t)\big]dt, \tag{1.17}$$

where $r > 0$ is a scalar weight parameter, subject to the dynamics of the system (1.16). It is assumed that $q : \mathbb{R}^n \to \mathbb{R}_+$ is a positive semi-definite function with the following properties. The dynamical system (1.16) with output $y = q(X)$ is zero-state detectable and $q(0) = 0$. Suppose that $u^*(x)$ is a minimizer of the optimal control problem and its corresponding value function $V : \mathbb{R} \times \mathbb{R}^n \to \mathbb{R}_+$ is given by

$$V = J(x_0),$$

which is a solution of the Hamilton-Jacobian-Bellman (HJB) equation

$$V_x{}^T f(x) - \frac{1}{4r} V_x{}^T g(x) g^T(x) V_x + q(x) = 0 \tag{1.18}$$

and $V_x = \nabla_x V$ is gradient of V with respect to x. Moreover, the optimal control policy for the nonlinear system (1.16) can be calculated explicitly via

$$u^*(x) = -\frac{1}{2r} g^T(x) V_x. \tag{1.19}$$

The HJB equation (1.18) is a partial differential equation that may not have a smooth closed-form solution in general; however, it is possible to be reformulated as a boundary value problem and be solved numerically. The main challenge is how to approximate the optimal solution (1.19) by finding approximate solutions for the HJB equation. In this part of the project, we apply the Carleman embedding technique to lift the HJB equation and represent the lifted HJB equation as an infinite-dimensional quadratic equation.

Before introducing our quadrization method for the HJB equation, we lift nonlinear control system (1.16) into a bilinear system. The analytic functions f and g can be represented by power series expansions

$$f(x) = \sum_{i=1}^{\infty} f_i \, x^{[i]} \tag{1.20}$$

and

$$g(x) = \sum_{i=0}^{\infty} g_i \, x^{[i]} \tag{1.21}$$

for all $\|x\| \leq R_0$, where $R_0 > 0$ is the convergence radius of these series. Despite the previous part of the project, we keep all the redundant monomials when performing lifting operation. To this end, we define the Kronecker power of a vector $x = [x_1, \ldots, x_n]^T$ by

$$x^{[i]} = \overbrace{x \otimes \cdots \otimes x}^{\text{i operands}} \in \mathbb{R}^{n^i}, \quad i \geq 1$$

and the Carleman lifting operator by

$$\Psi(x) := \mathrm{col}\big(x, x^{[2]}, x^{[3]}, \dots\big). \tag{1.22}$$

The nonlinear control system (1.16) can be represented as

$$\dot{\Psi} = \mathbf{A}\Psi + (\mathbf{B}\Psi + \mathbf{b}_0)u, \tag{1.23}$$

where

$$\mathbf{b}_0 = \begin{bmatrix} g_0 \\ 0 \\ 0 \\ \vdots \end{bmatrix}, \tag{1.24}$$

$$\mathbf{A} = \begin{bmatrix} A_1^1 & A_2^1 & A_3^1 & \dots & A_M^1 & A_{M+1}^1 & \dots \\ 0 & A_2^2 & A_3^2 & \dots & A_M^2 & A_{M+1}^2 & \dots \\ 0 & 0 & A_3^3 & \dots & A_M^3 & A_{M+1}^3 & \dots \\ \vdots & \vdots & \vdots & \ddots & & \ddots & \ddots \end{bmatrix}, \tag{1.25}$$

$$\mathbf{B} = \begin{bmatrix} B_1^1 & B_2^1 & B_3^1 & \dots & B_M^1 & B_{M+1}^1 & \dots \\ B_1^2 & B_2^2 & B_3^2 & \dots & B_M^2 & B_{M+1}^2 & \dots \\ 0 & B_2^3 & B_3^3 & \dots & B_M^3 & B_{M+1}^3 & \dots \\ \vdots & \vdots & \vdots & \ddots & & \ddots & \ddots \end{bmatrix}, \tag{1.26}$$

$$A_{i+j-1}^i = \sum_{v=1}^{i} \overbrace{\mathbb{I}_{n\times n} \otimes \cdots \otimes \underset{\substack{\uparrow \\ v\text{'th position}}}{f_j} \otimes \cdots \otimes \mathbb{I}_{n\times n}}^{\text{i times}}, \ i,j \geq 1, \tag{1.27}$$

and

$$B_{i+j-1}^i = \sum_{v=1}^{i} \overbrace{\mathbb{I}_{n\times n} \otimes \cdots \otimes \underset{\substack{\uparrow \\ v\text{'th position}}}{g_j} \otimes \cdots \otimes \mathbb{I}_{n\times n}}^{\text{i times}}, \ i \geq 1, j \geq 0. \tag{1.28}$$

1.2.2 Quadrization of the HJB Equation

By assuming that $q(x)$ in the cost function is an analytic function on a neighborhood of the origin and a nonnegative function with $q(0) = 0$, we have

$$q(x) \ = \ \sum_{i,j=1}^{\infty} x^{[i]^T} Q_j^i \, x^{[j]} \tag{1.29}$$

for all $\|x\| \leq R_0$, where $R_0 > 0$. Hence, we can rewrite $q(x)$ as

$$q(\Psi) = \Psi^T \mathbf{Q} \Psi, \tag{1.30}$$

where $\mathbf{Q}$ is a symmetric matrix with $\mathbf{Q}_{[ij]} = Q_{ij} \in \mathbb{R}^{n^i \times n^j}$.

Lemma 1.3. *Any positive function $V : \mathbb{R}^n \to \mathbb{R}$ that satisfies the lifted HJB equation will satisfy the original HJB equation as well.*

Theorem 1.4. *Suppose that the nonnegative weight function $q(x)$ is analytic and the corresponding HJB equation admits an analytic function as its solution in a neighborhood of the origin. If the semi-Riccati operator equation*

$$\mathbf{PA} + \mathbf{A}^T\mathbf{P} + \mathbf{Q} - \frac{1}{r}\Big(\mathbf{P}\mathbf{b}_0\mathbf{b}_0^T\mathbf{P} + \mathbf{C}\mathbf{C}^T + \mathbf{C}\mathbf{b}_0^T\mathbf{P} + \mathbf{P}\mathbf{b}_0\mathbf{C}^T\Big) = 0, \tag{1.31}$$

in which $\Psi^T\mathbf{P}\mathbf{B}\Psi = \mathbf{C}^T\Psi$, has a symmetric solution that is quadratically bounded over $\mathcal{S}$, then the value function of the optimal control problem can be expressed by

$$V(x_0) = \Psi(x_0)^T\mathbf{P}\Psi(x_0)$$

and the optimal control law by

$$u^*(x) = -\frac{1}{r}\left(\mathbf{B}\Psi + \mathbf{b}_0\right)^T\mathbf{P}\Psi \tag{1.32}$$

where $\mathbf{Q}$ is a symmetric matrix that satisfies $q(x) = \Psi(x)^T\mathbf{Q}\Psi(x)$.

We emphasize that the solution $\mathbf{P}$ may not be unique nor positive globally. However, we show that the resulting value function will behave as a Lyapunov function for the closed-loop system in a neighborhood of the origin.

1.2.3 Exact and Iterative Solution of the semi-Riccati Operator Equation

The operator equation (1.31) resembles the well-known Riccati equation; however, it is extremely complex because operator $\mathbf{P}$ is dissolved implicitly within operator $\mathbf{C}$. A brute force truncation will not result in a converging approximation of $\mathbf{P}$. Employing optimization methods to minimize finite truncation of the left-hand side of (1.31) will be computationally expensive and will not scale as a function of the truncation length. Our ideas is to use the block upper triangular structure of state matrices $\mathbf{A}$ and $\mathbf{B}$ as well as symmetry of $\mathbf{P}$. Our main contribution in this part is to propose a novel iterative method to calculate sub-blocks of operator $\mathbf{P}$ in an *exact* manner up to any arbitrary order. For every $N \geq 1$, let us denote the N'th order finite-section of operators $\mathbf{A}, \mathbf{B}$, $\mathbf{Q}$ by $\mathbf{A}_N, \mathbf{B}_N, \mathbf{Q}_N$, respectively.

Theorem 1.5. *If conditions*

a. *$(f_1, g_0$ is controllable and (Q_1^1, f_1) is observable,*

b. *the matrix* (1.35) *be invertible for all $j \geq 2$,*

c. *sub-blocks $-A_j^j$, A_i^i have no common eigenvalue for all $i, j \geq 2$*

hold, then the lifted HJB equation (1.31) *has a unique solution.*

By rewriting operator equation (1.31) in terms of its sub-blocks and decomposing terms involving each sub-block of $\mathbf{P}$, we end up with three types of equations.

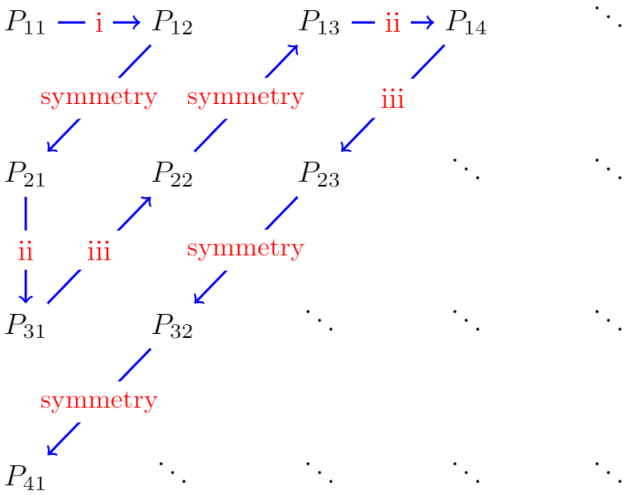

(a) This shows the order in which sub-blocks of $\mathbf{P}$ are calculated exactly and iteratively using one algebaric Riccati equation and a series of linear matrix equations.

(i) This type is for when $i = 1$, $j = 1$, which corresponds to the first sub-block of $\mathbf{P}$ and can be calculated through the finite-dimensional algebraic Riccati equation

$$P_1^1 A_1^1 + {A_1^1}^T P_1^1 - \frac{1}{r} P_1^1 g_0 g_0^T P_1^1 + Q_1^1 = 0. \tag{1.33}$$

This equation corresponds to the linear quadratic regulator of the first-order linearized system, where the condition (a) in Theorem (1.5) guarantees the existence of a unique positive definite solution P_1^1.

(ii) This type is for when $i = 1$ and $j \geq 2$. These are the remaining sub-blocks in the first row of operator $\mathbf{P}$, which can be calculated exactly through

$$P_j^1 A_j^j - \frac{1}{r} P_1^1 g_0 \Big(\overrightarrow{P_j^1 B_{(j-1)}^j}\Big)^T + \Big({A_1^1}^T - \frac{1}{r} P_1^1 g_0 g_0^T\Big) P_j^1 + H_j^1 = 0 \tag{1.34}$$

with

$$H_j^1 = Q_j^1 + \sum_{k=1}^{j-1} P_k^1 A_j^k - \frac{1}{r} \sum_{u=1}^{j-1} \sum_{k=1, k\neq j}^{u+1} P_1^1 g_0 \Big(\overrightarrow{P_k^{(j-u)} B_u^k}\Big)^T.$$

Equation (1.34) is a *linear* matrix equation and can be efficiently solved using vectorization techniques that are usually employed for solving the general Sylvester equation. If matrix

$$\mathcal{A}_j^1 = \Big(\mathbb{I}_{n^j} \otimes \big({A_1^1}^T - \frac{1}{r} P_1^1 g_0 g_0^T\big)^T\Big) + \Big({A_j^j}^T \otimes \mathbb{I}_n\Big) - \frac{1}{r}\Big(B_{(j-1)}^{j^T} \otimes \mathbb{I}_n \otimes P_1^1 g_0\Big) \tag{1.35}$$

is invertible, then (1.34) will have a unique solution.

(iii) This type is when $i \geq 2$ and $j \geq 2$. These are sub-blocks of operator $\mathbf{P}$ in the remaining rows, which can be calculated exactly through

$$P_j^i A_j^j + A_i^{i^T} P_j^i + H_j^i = 0 \tag{1.36}$$

with

$$H_j^i = Q_j^i + \sum_{k=1}^{j-1} P_k^i A_j^k + \sum_{k=1}^{i-1} A_i^{k^T} P_j^k - \frac{1}{r}\Bigg(P_1^i g_0 g_0^T P_j^1 + \sum_{u=1}^{i-1}\sum_{k=1}^{u+1} \Big(\overrightarrow{P_k^{(i-u)} B_u^k}\Big) g_0^T P_j^1 + \sum_{u=1}^{j-1}\sum_{k=1}^{u+1} P_1^i g_0 \Big(\overrightarrow{P_k^{(j-u)} B_u^k}\Big)^T + \sum_{u=1}^{i-1}\sum_{v=1}^{j-1}\sum_{k=1}^{u+1}\sum_{l=1}^{v+1} \Big(\overrightarrow{P_k^{(i-u)} B_u^k}\Big)\Big(\overrightarrow{P_l^{(j-v)} B_v^l}\Big)^T \Bigg).$$

Equation (1.36) is linear and has a unique solution if matrices A_i^i and $-A_j^j$ do not share any common eigenvalue.

Theorem 1.6. *If $g_0 = 0$ and all eigenvalues of f_1 have strictly negative real parts, then the semi-Riccati equation* (1.31) *will admit a unique symmetric solution.*

Figure 1.1a shows the order in which calculation of sub-blocks of $\mathbf{P}$ is carried out. We emphasize that our method calculates the exact sub-blocks of the solution of the semi-Riccati operator equation. This is different from an approximate solution that one may obtain by solving a truncated version of the semi-Riccati equation (1.31). Our method is efficient and computationally tractable as it involves solving one algebaric Riccati equation and a series of linear matrix equations.

1.3 Systemic Risk Analysis of Networked Systems

In this part of the project, we consider a class of nonlinear cooperative networks, which consist of multiple agents that are coupled together via an undirected state-dependent graph. We develop a representation of the system solution by decomposing the nonlinear system utilizing ideas from the Koopman operator theory and its spectral analysis. We use recent results on the extensions of the well-known Hartman theorem for hyperbolic systems to establish a connection between the original nonlinear dynamics and the linearized dynamics in terms of Koopman spectral properties. The expected value of the output energy of the nonlinear network, which is related to the notions of coherence and robustness in dynamical networks, is evaluated and characterized in terms of Koopman eigenvalues, eigenfunctions, and modes. Spectral representation of the risk measure enables us to develop algorithmic methods to assess the risk of this class of nonlinear dynamical networks as a function of their graph topology. Finally, we propose a scalable computational method for approximation of the components of the Koopman mode decomposition, which is necessary to evaluate the systemic risk measure of the nonlinear dynamical network. The details of research achievements in this part can be found in [22].

We consider the class of dynamical system whose evolution is governed by

$$\dot{\mathbf{x}} = \mathbf{F}(\mathbf{x}), \tag{1.37}$$

with $\mathbf{F}(\mathbf{x}) : \mathbb{R}^{\mathbf{n}} \to \mathbb{R}^{\mathbf{n}}$ representing a C^2 vector field on $\mathbb{R}^n$. For the initial condition $\mathbf{x_0} \in \mathbb{R}^{\mathbf{n}}$, $\mathbf{x(t)} := \mathbf{S(t, x_0)} : \mathbb{R}_+ \times \mathbb{R}^{\mathbf{n}} \to \mathbb{R}^{\mathbf{n}}$ is the generated flow of (1.37), which is assumed to be defined for all $t \geq 0$. We assume that $\mathbf{F}$ attains a hyperbolic stable fixed point at the origin. i.e., $\mathbf{F(0)} = \mathbf{0}$. Moreover, we denote the Jacobian of $\mathbf{F}$ at the fixed point by

$$\mathbf{A} := \frac{\partial}{\partial \mathbf{x}} \mathbf{F}|_{\mathbf{x=0}}, \tag{1.38}$$

which we assume to be Hurwitz; i.e., the eigenvalues of $\mathbf{A}$ have strictly negative real parts. The basin of attraction of the origin is an open neighborhood of $\mathbf{0}$ with $\Omega \subset \mathbb{R}^n$ a compact subset of this neighborhood. By definition, $\mathbf{S}(t, \mathbf{x_0}) \in \mathbf{\Omega}$ for any $\mathbf{x_0} \in \mathbf{\Omega}$ and $t \geq 0$, such that $\mathbf{S}(\mathbf{t}, \mathbf{x_0}) \to \mathbf{0}$ as $t \to +\infty$. Let us define the functional space

$$\mathcal{F} = \Big\{ f \in C^1(\Omega, \mathbb{R}) \;\Big|\; |f|_{C^1} < \infty \Big\} \tag{1.39}$$

that together with norm $|f|_{C^1} := \sup_{\mathbf{x}\in\mathbf{\Omega}} \big|f(\mathbf{x})\big| + \sup_{\mathbf{x}\in\mathbf{\Omega}} \big\|\nabla \mathbf{f}(\mathbf{x})\big\|$, constitute a Banach space. This will be the space of observable functions on flow $\mathbf{S}(\cdot, \mathbf{x_0})$. For fixed $t \geq 0$, the Koopman operator $U^t : \mathcal{F} \to \mathcal{F}$ associated with (1.37) is

$$(U^t f)(\mathbf{x_0}) = f \circ \mathbf{S}(t, \mathbf{x_0}). \tag{1.40}$$

For any fixed $t \geq 0$, it can be shown that U^t is linear in $\mathcal{F}$. Furthermore, the collection $\{U^t\}_{t\geq 0}$ constitutes a semigroup known as the Koopman semigroup. In the context of continuous autonomous dynamical systems, (1.40) is interpreted as the action of semigroup on observable $f \in \mathcal{F}$. The spectrum of operator U^t may consist of a discrete, continuous and residual part. The discrete part, also known as point spectrum of U^t, is defined as

$$\sigma_p(U^t) = \big\{ \lambda \in \mathbb{C} \,\big|\, U^t\phi = e^{\lambda t}\phi, \text{ for some } \phi = \phi_\lambda \in \mathcal{F} \big\}. \tag{1.41}$$

Throughout this report $\big(\lambda, \phi_\lambda\big)$, for $\lambda \in \sigma_p(U^t)$, is called the Koopman pair of an eigenvalue with its corresponding eigenfunction. Our goal is to highlight the role of the spectral operator theory in evaluating quadratic risk measures for a class of nonlinear consensus protocols that enjoy a great interest in the field of networked control systems. More specifically, we leverage a recent extension of the Hartman's theorem for hyperbolic dynamical systems to outline the pivotal role of point spectrum in approximating the output energy of nonlinear distributed cooperative algorithms.

We apply the extension of the Hartman's theorem in order to investigate the conditions under which one is able to express the flow of the system in terms of the Koopman pairs. We use an interesting fact about the map created by stacking specific eigenfunctions of the Koopman operator and its inverse map for dynamical systems with hyperbolic stable fixed points: polynomial approximations of the inverse map yields a Koopman Mode Decomposition.

The celebrated theorem of Hartman establishes a crucial connection between autonomous dynamical system (1.37) and the dynamics of the linearized system around the origin. A moment of reflection can lay the groundwork of bridging the gap between spectral properties of the nonlinear and the linearized system around the fixed point. Let us consider dynamical system (1.37) with the smoothness assumptions on $\mathbf{F}$ to hold and the origin to be a hyperbolic fixed point. Then, there exists a C^1-diffeomorphism $\mathbf{H}$ of a neighborhood U of the origin on an open set $\Omega' \subset \Omega$ containing the origin such that for each $\mathbf{x_0} \in \Omega'$, there exists is an open interval $I(\mathbf{x}_0) \subset \mathbb{R}_+$ containing zero such that for all $\mathbf{x_0} \in U$ and $t \in I(\mathbf{x_0})$

$$\mathbf{H} \circ \mathbf{S}(\mathbf{t}, \mathbf{x_0}) = \mathrm{e}^{\mathbf{At}}\, \mathbf{H}(\mathbf{x_0}),$$

where $\mathbf{A} = \frac{\partial}{\partial \mathbf{x}}\mathbf{F}|_{\mathbf{x}=\mathbf{0}}$. This has been extended by other researchers to hold true over the whole the basin of attraction of the fixed point at the origin. More precisely, if $\mathbf{F}$ is C^2 and $\mathbf{A} = \frac{\partial}{\partial \mathbf{x}}\mathbf{F}|_{\mathbf{x}=0}$ is Hurwitz, then there exists a diffeomorphism $\alpha : \Omega \to \mathbb{R}^n$ such that

$$\alpha \circ \mathbf{S}(\mathbf{t}, \mathbf{x_0}) = \mathrm{e}^{\mathbf{At}}\, \alpha(\mathbf{x_0}), \tag{1.42}$$

for all $\mathbf{x_0} \in \Omega$ and $t \geq 0$. By assuming that $\mathbf{A}$ is diagonalizable, we can write $\mathbf{A} = \mathbf{R\Lambda R^{-1}}$ where Λ is a diagonal matrix, having diagonal elements with strictly negative real parts. Let us define

$$\mathbf{H}(\mathbf{x}) := \mathbf{R^{-1}}\alpha(\mathbf{x}). \tag{1.43}$$

Then, we observe that

$$\mathbf{H}\left(\mathbf{S}(\mathbf{t}, \mathbf{x_0})\right) = \mathbf{R^{-1}}\mathrm{e}^{\mathbf{At}}\mathbf{R}\mathbf{H}(\mathbf{x_0}) = \mathrm{e}^{\mathbf{\Lambda t}}\mathbf{H}(\mathbf{x_0}). \tag{1.44}$$

Clearly, map $\mathbf{H} : \mathbf{\Omega} \to \mathbb{C}^{\mathbf{n}}$ is a diffeomorphism. Hence, flow of the dynamical system $\mathbf{S}(\cdot, \mathbf{x_0})$ can be expressed as

$$\mathbf{S}(\mathbf{t}, \mathbf{x_0}) = \mathbf{H^{-1}}\left(\mathrm{e}^{\mathbf{\Lambda t}}\mathbf{H}(\mathbf{x_0})\right), \quad \text{for every } \mathbf{t} \geq \mathbf{0} \text{ and } \mathbf{x_0} \in \mathbf{\Omega}. \tag{1.45}$$

This suggests that knowledge of maps $\mathbf{H}$ and $\mathbf{H}^{-1}$ helps identify the flow of the system. In an interesting turn of events, there is an important correlation between Koopman spectrum and the eigenvalues of the Jacobian matrix at the fixed point $\mathbf{A}$.

Theorem 1.7. *Let map* $\mathbf{H}$ *given in* (1.43) *have component-wise expression*

$$\mathbf{H} = \left[H_1, H_2, \ldots, H_n\right]^T, \tag{1.46}$$

for $H_i : \Omega \to \mathbb{C}^n$ *and* $i = 1, \ldots, n$. *If* λ_i *is the i-th eigenvalue of* $\mathbf{A}$, *then* $\left(\lambda_i,\, H_i\right)$ *is a pair of Koopman eigenvalue and its corresponding eigenfunction.*

In the virtue of the Stone-Weierstrass theorem, $\mathbf{H}^{-1}(\mathbf{x})$ can be uniformly ϵ-approximated over the domain of $\mathbf{H}^{-1}$ by multivariate polynomials. Therefore, for every $\mathbf{x} \in \mathrm{dom}\,\mathbf{H^{-1}}$ we can write

$$\mathbf{H}^{-1}(\mathbf{x}) \overset{\epsilon}{\approx} \sum_{\gamma \in \Gamma_\epsilon} \mathbf{c}_\gamma^\epsilon \; x_1^{j_1} \cdots x_n^{j_n}, \tag{1.47}$$

where $\gamma = [j_1, \ldots j_n]^T \in \mathbb{Z}_+^n$, $\overset{\epsilon}{\approx}$ implies the approximation with maximal error of ϵ, and $\mathbf{c}_\gamma^\epsilon = \mathbf{c}_{j_1,\ldots j_n}^\epsilon$ is represented using the multi-index notation. The index set $\Gamma_\epsilon \subset \mathbb{Z}_+^n$ consists of finite number of indices based on the desired level of accuracy $\epsilon > 0$. If map $\mathbf{H^{-1}}$ is analytic, then it admits a Maclaurin expansion with a positive radius of convergence and we can have an infinite series representation (at least in a subset of Ω^{-1}) similar to (1.47). We highlight that not every polynomial approximation of $\mathbf{H}^{-1}$ is suitable for our purpose. It is necessary for the right-hand side of (1.47) to vanish at the origin, as $\mathbf{H}^{-1}$ does as well. This property permits a credible polynomial approximation of the output energy of (1.37) in terms of Koopman modes. Examples of polynomial expansions that can approximate $\mathbf{H^{-1}}$ under such constraints are interpolation based methods using multi-variate polynomials of the Bernstein or Chebyshev families, with appropriate scaling of domain of $\mathbf{H^{-1}}$.

Theorem 1.8. *Let* $\mathbf{A} = \frac{\partial}{\partial \mathbf{x}}\mathbf{F}(\mathbf{x})|_{\mathbf{x}=\mathbf{0}}$ *be diagonalizable and Hurwitz with eigenvalues* $\lambda_1, \ldots, \lambda_n$. *Consider map* $\mathbf{H^{-1}}(\mathbf{x})$ *with elements given* (1.43) *for every* $\mathbf{x_0} \in \mathbf{\Omega}$, *where* Ω *is a compact set. Then, using the approximation* (1.47) *for* $\mathbf{H}^{-1}(\mathbf{x})$, *flow* $\mathbf{S}(\cdot, \mathbf{x}_0)$ *of nonlinear system* (1.37) *attains the representation*

$$\mathbf{S}(t, \mathbf{x}_0) \overset{\epsilon}{\approx} \sum_{i \geq 1} \mathbf{c}_i \, \mathrm{e}^{\bar{\lambda}_i t}\phi_i(\mathbf{x}_0), \qquad \textit{for all } t \geq 0$$

where for the ordered vector $\gamma_i = [j_1, \ldots, j_n]^T \in \Gamma_\epsilon \subset \mathbb{Z}_+^n$, *we have*

$$\bar{\lambda}_i := \sum_{k=1}^{n} j_k \lambda_k \quad \textit{and} \quad \phi_i(\mathbf{x}_0) := \prod_{k=1}^{n} H_k^{j_k}(\mathbf{x}_0). \tag{1.48}$$

This result enables us to characterize several risk and performance measure in nonlinear dynamical networks in terms of spectrum of the underlying graph of the network. To illustrate effectiveness of our proposed method, we can consider characterizing a risk measure for a class of nonlinear consensus networks whose dynamics are governed by

$$\dot{x}_i = \sum_{\{i,j\}\in\mathcal{E}} w_{ij}\,(x_j - x_i), \tag{1.49}$$

where $\mathcal{E}$ is the set of edges of the undirected graph of the network whose weights are symmetric and state-dependent in the form of

$$w_{ij} = w_{ji} = \tilde{w}_{ij}\, g\left(|x_i - x_j|^2\right), \tag{1.50}$$

for $g : \mathbb{R}_+ \to \mathbb{R}_{++}$ a positive coupling function of the graph, and constant $\tilde{w}_{ij} > 0$. We note that such a state-dependence of the couplings is motivated by a natural assumption: the remote or dissimilar agents less likely interact with each other. For instance, this is the case in the context of social networks, oscillatory networks or biological networks. For this reason, function g is usually considered to be monotonically decreasing. By defining the state of the network as $\mathbf{x} := [x_1, \ldots, x_n]^T \in \mathbb{R}^n$, we may express the collective dynamics of the agents as

$$\dot{\mathbf{x}} = -\mathcal{L}_{\mathbf{x}}\,\mathbf{x} \tag{1.51}$$

where $\mathcal{L}_{\mathbf{x}}$ is the state-dependent graph Laplacian matrix with coupling weights that vary according to (1.50). Our analysis relies on two assumptions: (1) The function g is analytic and it satisfies $g(0) = 1$, (2) the graph with coupling weights $\{\tilde{w}_{ij}\}_{\{i,j\}\in\mathcal{E}}$ is connected. The average of $\mathbf{x_0}$ is called the consensus equilibrium of the network over the state of interest. By considering observable $\mathbf{y}(t, \mathbf{y}_0) = \mathbf{M}_n\,\mathbf{S}(t, \mathbf{x}_0)$, $t \geq 0$ for the network, where $\mathbf{M}_n$ is the centering matrix, the energy of the output once weighted with a positive-definite and symmetric matrix $\mathbf{Q}$ is

$$\int_0^\infty \mathbf{y}^T(t, \mathbf{y}_0)\mathbf{Q}\ \mathbf{y}(t, \mathbf{y}_0)\, dt.$$

We choose the risk measure as the mean energy of the vanishing signal $\mathbf{y}$, when the state of the consensus system starts from a random initial condition $\mathbf{x_0}$. The long term energy of the output signal $\mathbf{y}$ that converges to zero is equivalent to the energy of the state vector $\mathbf{x}$ to converge to consensus. We take this mean for uncertain initial conditions, by assuming that the initial state is a random variable $\mathbf{x}_0 : \Omega_s \to \Omega$ from the sample space Ω_s, with some probability measure (e.g. a probability density function or a probability mass function). In either case, we define the risk measure as

$$\rho\,(\mathcal{L}) := \mathbb{E}_{\mathbf{x}_0}\left\{\int_0^\infty \mathbf{S}^T(t, \mathbf{x}_0)\mathbf{M}_n^T\mathbf{Q}\ \mathbf{M}_n\mathbf{S}(t, \mathbf{x}_0)\, dt\right\}. \tag{1.52}$$

The next result establishes an analytical expression for the risk measure of that reflects the contributions of the spectra of the linearized graph Laplacian and eigenfunctions of the Koopman operator.

Theorem 1.9. *Let us consider the corresponding disagreement dynamics of* (1.51) *and the associated flow* $\mathbf{S}(\cdot, \mathbf{y}_0)$ *for all initial disagreements* $\mathbf{y}_0$*. Then, the risk measure* (1.52) *can be expressed as*

$$\rho(\mathcal{L}) = \sum_{i,j\geq 1} \phi_{ij} c_{ij} \frac{1}{\bar{\lambda}_i + \bar{\lambda}_j}, \tag{1.53}$$

where $\{\bar{\lambda}_i\}_{i=1,2,\dots}$ *is the sequence of Koopman eigenvalues in the Koopman Mode Decomposition, enumerated by an arbitrary numbering of* $\gamma_i = (j_2, \dots, j_n) \in \mathbb{Z}_+^{n-1}$ *as*

$$\bar{\lambda}_i := \sum_{k=2}^{n} j_k \lambda_k \quad \textit{and} \quad \phi_i(\mathbf{x}_0) := \prod_{k=2}^{n} H_k^{j_k}(\mathbf{x}_0).$$

with $\lambda_2, \dots, \lambda_n$ *being the nonzero eigenvalues of* $\mathcal{L}_{\mathbf{0}} := \frac{\partial}{\partial \mathbf{x}} \mathcal{L}(\mathbf{x})|_{\mathbf{x}=0}$. *Moreover,* $\phi_{ij} := \mathbb{E}_{\mathbf{x}_0}\{\phi_i(\mathbf{y})\phi_j(\mathbf{y})\}$ *and* $c_{ij} := \mathbf{c}_i^T Q\, \mathbf{c}_j$, *are computed in terms of Koopman eigenfunctions and modes, respectively.*

The significance of our result is that now it is possible to investigate effect of interconnection topology (Laplacian eigenvalues) on the value of the risk measure and utilize that to design robust nonlinear dynamical networks. We highlight that various systemic risk measures can be considered; however, one may not be able to quantify those risk measure explicitly in terms of Laplacian eigenvalues.

1.4 Discussion of Other Research Achievements

1.4.1 Systemic Risk of Collision in Vehicle Platooning: Hard Limits and Tradeoffs

In [24, 23, 17, 16, 18], we quantify the value-at-risk of inter-vehicle collision and detachment for a class of platoons, in presence of communication time-delay and stochastic noise. Closed-form expressions for the risk measures are obtained as functions of Laplacian eigen-spectrum as well as their explicit approximations. We quantify several hard limits and fundamental tradeoffs among the risk measures, network connectivity, communication time-delay, and statistics of exogenous stochastic noise. Simultaneous presence of noise and time-delay in a platoon reveals an idiosyncratic behavior risk of collision and detachment, for instance, weakening (improving) network connectivity may result in lower (higher) levels of risk.

1.4.2 Aggregate Fluctuations in Networks Driven by Stable Non-Gaussian Noise

In [26], we quantify measures of aggregate fluctuations for consensus-seeking networks subject to exogenous noise with -stable distributions. This type of noise is generated by a class of random measures with heavy-tailed probability distributions. We define a cumulative-scale parameter over the output variables, as a measure of aggregate fluctuation. We show that this class of measures can be characterized implicitly, because finding its explicit form in terms of network parameters is, in general, almost impossible. To this end, we offer several tractable upper bounds in terms of Laplacian spectrum and statistics of the input noise. Our results suggest that relying on Gaussian-based optimal design algorithms will result in non-optimal solutions for dynamical networks that operate in the face of non-Gaussian noise.

1.4.3 Risk of Phase Incoherence in Wide Area Control of Power Networks

In [27, 25], we develop a framework to quantify systemic risk measures in a class of Wide-Area-Control (WAC) policies in power systems in the presence of noisy and timedelayed sensory data. A closed-form calculation of the risk of phase incoherence in interconnected power networks is presented, and the effect of network parameters, information flow in WAC architecture, statistics of noise, and time delays are characterized. We show that in the presence of time-delay and noise, a fundamental trade-off between the best achievable performance (via tuning feedback gains) and value-at-risk emerges. The significance of our results is that they provide a guideline for developing

algorithmic design tools to enhance the coherency and robustness of closed-loop power networks simultaneously.

1.4.4 Risk-aware learning of recurrent neural networks in presence of exogenous noise

In [1, 2], it is discussed that Recurrent Neural networks (RNN) have shown promising potential for learning dynamics of sequential data. However, artificial neural networks are known to exhibit poor robustness in presence of input noise, where the sequential architecture of RNNs exacerbates the problem. In this paper, we will use ideas from control and estimation theories to propose a tractable robustness analysis for RNN models that are subject to input noise. The variance of the output of the noisy system is adopted as a robustness measure to quantify the impact of noise on learning. It is shown that the robustness measure can be estimated efficiently using linearization techniques. Using these results, we proposed a learning method to enhance robustness of a RNN with respect to exogenous Gaussian noise with known statistics.

1.4.5 Risk of Misclassification in Recurrent Neural Networks with Noisy Inputs

In [13, 14, 15], we develop a classification framework using recurrent neural networks (RNN) that exhibits robust performance in the presence of input perturbations. It is shown that by requiring the RNN to be stable, we can quantify a series of explicit error bounds in terms of trainable weight matrices and guarantee convergence of the proposed classification method. Furthermore, the stability and convergence conditions impose some norm bounds on the trainable weight matrices that can be used as constraints during the learning process. The effectiveness of our proposed method has been validated using extensive simulations on map and image classification problems.

1.4.6 Statistical Learning of Interactions in Nonlinear Dynamical Networks

In [9, 8], we develop a methodology to learn dynamics of a class of second-order networks through their interaction kernels. Important applications include formation control in a swarm of robots and platooning of autonomous vehicles. It is shown that under some reasonable assumptions the governing stochastic dynamics of such networks will generate geometrically ergodic trajectories. This property allows us to learn interaction kernels of a general class of dynamical networks using only one single sample trajectory, which makes our results practically plausible as it is either impossible or expensive to repeat an experiment to collect enough data for training. Furthermore, we build upon ideas from the concentration inequalities for geometrically ergodic Markov chains and prove that our proposed learning method converges with semi-exponential rate to the optimal solution within a compact and convex set of hypothesis functions.

1.4.7 Estimation with fast feature selection in robot visual navigation

In [20], we consider the robot localization problem with sparse visual feature selection. The underlying key property is that contributions of trackable features (landmarks) appear linearly in the information matrix of the corresponding estimation problem. We utilize standard models for motion and vision system using a camera to formulate the feature selection problem over moving finite-time horizons. We propose a scalable randomized sampling algorithm to select more informative features to obtain a certain estimation quality. We provide probabilistic performance guarantees for our method. The time-complexity of our feature selection algorithm is linear in the number of candidate features, which is practically plausible and outperforms existing greedy methods that scale quadratically with the number of candidate features. Our numerical simulations confirm that not only the

execution time of our proposed method is comparably less than that of the greedy method, but also the resulting estimation quality is very close to the greedy method.

1.4.8 Localized stability certificates for spatially distributed systems

In [19], we focus on localized conditions to verify exponential stability of spatially distributed linear systems whose interconnection structures are defined using a geodesic on proximity coupling graphs. We reformulate the exponential stability condition in the form of a feasibility condition that is amenable to localized implementations. Using finite truncation techniques, we obtain decentralized necessary and sufficient stability certificates. In order to guarantee global stability, it suffices to certify localized conditions over a graph covering, where the computational complexity of the verification of the proposed localized certificate is independent of network size. Several robustness conditions against local matrix perturbations are obtained that are useful for tuning network parameters in a decentralized manner while ensuring global exponential stability.

References

[1] Arash Amini, Guangyi Liu, and Nader Motee. Robust learning of recurrent neural networks in presence of exogenous noise. In *2021 60th IEEE Conference on Decision and Control (CDC)*. IEEE, 2021.

[2] Arash Amini, Guangyi Liu, and Nader Motee. Robust learning of recurrent neural networks in presence of exogenous noise. **IEEE Transactions on Automatic Control**, 2021. Under Review.

[3] Arash Amini, Hossein K. Mousavi, Sun Qiyu, and Nader Motee. Space-time sampling for network observability. **IEEE Transactions on Automatic Control**, 2020. Under Review.

[4] Arash Amini, Qiyu Sun, and Nader Motee. Carleman state feedback control design of a class of nonlinear control systems. *IFAC-PapersOnLine*, 52(20):229–234, 2019.

[5] Arash Amini, Qiyu Sun, and Nader Motee. Approximate optimal control design for a class of nonlinear systems by lifting hamilton-jacobi-bellman equation. In *2020 American Control Conference (ACC)*, pages 2717–2722. IEEE, 2020.

[6] Arash Amini, Qiyu Sun, and Nader Motee. Quadratization of hamilton-jacobi-bellman equation for near-optimal control of nonlinear systems. In *2020 59th IEEE Conference on Decision and Control (CDC)*, pages 731–736. IEEE, 2020.

[7] Arash Amini, Qiyu Sun, and Nader Motee. Error bounds for carleman linearization of general nonlinear systems. In *2021 Proceedings of the Conference on Control and its Applications*, pages 1–8. SIAM, 2021.

[8] Arash Amini, Qiyu Sun, and Nader Motee. Learning interaction kernels in swarm of agents from a single sample trajectory. In *American Control Conference*. Atlanta, Georgia, USA, 2022. Under Review.

[9] Arash Amini, Qiyu Sun, and Nader Motee. Learning potential-function-based interactions in swarm of agents using a single sample trajectory. In *L4DC 2022: Learning for Dynamics and Control Conference*. Stanford, CA., 2022. Under Review.

[10] Arash Amini, Cong Zheng, Qiyu Sun, and Nader Motee. Carleman linearization of nonlinear systems and their finite-section approximations. **SIAM Journal on Applied Dynamical Systems**, 2021. Under Review.

[11] Shima Dezfulian, Yaser Ghaedsharaf, and Nader Motee. Performance analysis and optimal design of time-delay directed consensus networks. **IEEE Transactions on Control of Network Systems**, 2022, In Press.

[12] Yaser Ghaedsharaf, Milad Siami, Christoforos Somarakis, and Nader Motee. Centrality in time-delay consensus networks with structured uncertainties. **Automatica**, 125:109378, 2021.

[13] Guangyi Liu, Arash Amini, Martin Takávc, and Nader Motee. Classification-aware path planning of network of robots. In *International Symposium Distributed Autonomous Robotic Systems*, pages 294–305. Springer, 2021.

[14] Guangyi Liu, Arash Amini, Martin Takávc, and Nader Motee. Robust classification using recurrent neural networks with perturbed sequential input data. In *American Control Conference*. Atlanta, Georgia, USA, 2022. Under Review.

[15] Guangyi Liu, Arash Amini, Martin Takac, and Nader Motee. Robust multi-agent classification with noisy sequential input data. **IEEE Transactions on Neural Networks and Learning Systems**, 2022. Under Review.

[16] Guangyi Liu, Vivek Pandey, Christoforos Somarakis, and Nader Motee. Risk of cascading failures in multi-agent rendezvous with communication time delay. In *American Control Conference*. Atlanta, Georgia, USA, 2022. Under Review.

[17] Guangyi Liu, Christoforos Somarakis, and Nader Motee. Risk of cascading failures in time-delayed vehicle platooning. In *2021 60th IEEE Conference on Decision and Control (CDC)*. IEEE, 2021.

[18] Guangyi Liu, Christoforos Somarakis, and Nader Motee. Risk of cascading failures in platoon of autonomous vehicles with delayed communication. In *IFAC Conference on Networked Systems (NecSys)*. Zurich, Switzerland, 2022. Under Review.

[19] Nader Motee and Sun Qiyu. Localized stability certificates for spatially distributed systems with sparse graph topologies. **SIAM Journal on Control and Optimization**, 2022.

[20] Hossein K Mousavi and Nader Motee. Estimation with fast feature selection in robot visual navigation. **IEEE Robotics and Automation Letters**, 5(2):3572–3579, 2020.

[21] Hossein K. Mousavi and Nader Motee. Explicit characterization of performance of a class of networked linear control systems. **IEEE Transactions on Control of Network Systems**, 7(4):1688–1699, 2020.

[22] Hossein K. Mousavi, Christoforos Somarakis, Qiyu Sun, and Nader Motee. Koopman performance analysis of nonlinear consensus networks. *In: Mauroy A., Mezić I., Susuki Y. (eds) The Koopman Operator in Systems and Control.* **Lecture Notes in Control and Information Sciences**, 484(10):523–551, 2020.

[23] Christoforos Somarakis, Yaser Ghaedsharaf, and Nader Motee. Risk of collision and detachment in vehicle platooning: Time-delay–induced limitations and tradeoffs. **IEEE Transactions on automatic control**, 65(8):3544–3559, 2019.

[24] Christoforos Somarakis, Yaser Ghaedsharaf, and Nader Motee. Time-delay origins of fundamental tradeoffs between risk of large fluctuations and network connectivity. **IEEE Transactions on Automatic Control**, 64(9):3571–3586, 2019.

[25] Christoforos Somarakis, Guangyi Liu, and Nader Motee. Risk of phase incoherence in wide area control of synchronous power networks. **IEEE Transactions on Automatic Control**, 2021. Under Review.

[26] Christoforos Somarakis and Nader Motee. Aggregate fluctuations in networks with drift-diffusion models driven by stable non-gaussian disturbances. **IEEE Transactions on Control of Network Systems**, 7(3):1248–1258, 2020.

[27] Christoforos Somarakis and Nader Motee. Delay-aware risk analysis and control in smart grid networks with corrupted measurements. In *2020 American Control Conference (ACC)*, pages 508–513. IEEE, 2020.